Observations of upwelling and relaxation events in the northern Monterey Bay during August 2000

Steven R. Ramp,[1] Jeffrey D. Paduan,[1] Igor Shulman,[2] John Kindle,[2] Frederick L. Bahr,[1] and Francisco Chavez[3]

Received 18 June 2004; revised 23 February 2005; accepted 31 March 2005; published 20 July 2005.

[1] The interplay between the Point Año Nuevo upwelling center, an offshore anticyclonic mesoscale eddy, and the waters of the Monterey Bay was studied during a series of up- and downwelling favorable wind events during August 2000. The upwelling events were characterized by the appearance of cold, salty water at Point Año Nuevo at the north end of the bay that subsequently spread southward across the mouth of the bay as the winds continued. During the downwelling/relaxation events, the surface current and temperature response was dominated by the onshore translation of the offshore eddy and by local surface heating in the bay itself. The circulation within the bay was cyclonic during both wind regimes but slightly more barotropic under poleward forcing. The ICON model, a nested, data assimilating, sigma coordinate model, was used to simulate the upwelling and relaxation events and calculate the subsurface current and density fields. The model reproduced the dominant current and temperature patterns outside the bay, including the southward flowing upwelling filament, the movement of the offshore eddy, the poleward flow off Point Sur, and the circulation within the bay. The model salinity fields at the surface and 100 m levels show that during upwelling, the bay was filled with higher-salinity water stemming from the Point Año Nuevo upwelling center to the north. During downwelling, the source water for both the surface and 100 m levels was the colder, fresher California Current water offshore, which had advected southward well past Point Piños during the previous upwelling event.

Citation: Ramp, S. R., J. D. Paduan, I. Shulman, J. Kindle, F. L. Bahr, and F. Chavez (2005), Observations of upwelling and relaxation events in the northern Monterey Bay during August 2000, *J. Geophys. Res.*, *110*, C07013, doi:10.1029/2004JC002538.

1. Introduction

[2] Over the past decade, the Monterey Bay has emerged as the locus of observational effort for a dozen or so oceanographic institutions located near its shores. Initially, these observations were of excellent quality but tended to be somewhat disparate, with each institution going their own way in search of physical, biological, surf zone, or operational insights. The Autonomous Ocean Sensing Network (AOSN) during August 2000 was an attempt to integrate across disciplinary lines using a cohesive, real-time data collection, data assimilation, and modeling and prediction effort. The bay is an attractive site for this project due to the presence of the Monterey Bay Submarine Canyon (MSC), which allows ready access to deep water, abrupt topography, and an ample continental shelf all within an easy day's steam from Monterey, Moss Landing, or Santa Cruz, California (Figure 1).

[3] The Naval Postgraduate School (NPS) provided the physical context for the AOSN program via (1) analysis of existing data sets in the Monterey Bay and (2) initiating new observational and numerical modeling efforts during August 2000 (Figure 1). The new observations consisted of (1) quasi-daily aircraft overflights to observe the air temperature, dew point temperature, wind speed and direction, and sea surface temperature (SST) in and above the bay; and (2) a bottom mounted acoustic Doppler current profiler (ADCP) that reported hourly current profiles in real time via an acoustic modem/radio frequency communications link. By flying below the quasi-permanent summertime stratus deck, the aircraft provided the spatial context for the in situ observations with a consistency, accuracy, and resolution not previously available from satellites. The ADCP, moored near the inshore edge of the Año Nuevo upwelling center, along with other buoys already moored elsewhere in the bay, revealed the vertical extent of the surface features observed by the aircraft. This combination of remote and in situ observations proved to be a powerful technique for understanding the local air/sea interaction processes in and around the Monterey Bay. The model used in this study was the 1–4 km resolution hydrodynamic model of the central California coast

[1]Department of Oceanography, Naval Postgraduate School, Monterey, California, USA.
[2]Oceanography Division, Naval Research Laboratory, Stennis Space Center, Mississippi, USA.
[3]Monterey Bay Aquarium Research Institute, Moss Landing, California, USA.

0148-0227/05/2004JC002538$09.00

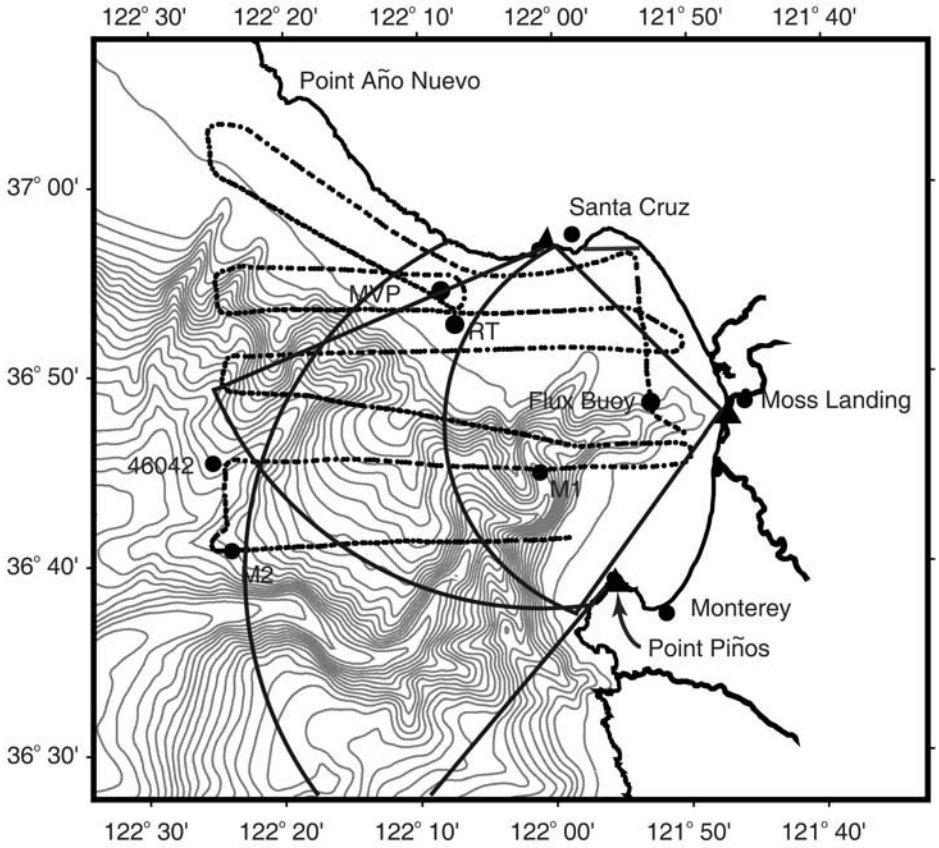

Figure 1. Locator map for the August 2000 observations. The dotted line indicates the aircraft flight track flown at an altitude of 130 m. The solid pie-shaped wedges show the coverage area for the three CODAR SeaSondes located at Point Piños, Moss Landing, and Santa Cruz. Moored buoy positions are indicated by the black dots and labeled accordingly. (RT, NPS real-time mooring; MVP, MBARI vertical profiler; Flux Buoy, NPS flux buoy; 48042, NOAA offshore buoy; M1, M2, MBARI surface moorings.)

developed under the ICON project [*Shulman et al.*, 2002]. The ICON model was nested within the Pacific West Coast (PWC) model [*Haidvogel et al.*, 2000], which was critically important in transferring the remote forcing along the coast to the smaller subdomain.

2. Background

[4] The mesoscale variability near the Monterey Bay can be succinctly described as the interplay between the upwelling filaments rooted at headlands to the north and south of the bay and a persistent, anticyclonic California Current meander just offshore of the bay itself. The upwelling centers at Point Año Nuevo to the north and Point Sur to the south are clearly driven by the prevailing northwesterly winds, which are strongest during March through June [*Nelson*, 1977]. The flow off Año Nuevo was well described using CTD and AVHRR data during two brief periods in May and June 1989 [*Rosenfeld et al.*, 1994]. They found a bifurcated flow off Año Nuevo, with some of the cold, salty upwelled water flowing offshore and some flowing south over the Monterey Canyon. This flow from the north was found to be the primary source of cold water over the canyon, and the authors disputed earlier claims [*Bigelow and Leslie*, 1930; *Bolin and Abbott*, 1963; *Breaker and Gilliland*, 1981] that the cold water in the center of the bay stems from upwelling within the canyon itself. Tidally driven upwelling near the canyon rim may move out of the canyon and along the bottom over the continental shelf, particularly on the southern side of the canyon [*Petruncio et al.*, 1998] but there is no hard evidence that this water ever reaches the surface.

[5] To the south of the bay, another strong upwelling center located at Point Sur also generates cold near-surface filaments moving offshore [*Breaker and Mooers*, 1986; *Tisch et al.*, 1992; *Rosenfeld et al.*, 1994; *Ramp et al.*, 1997]. On the continental shelf there, currents were equatorward during northwesterly winds and poleward during wind reversals and relaxations [*Ramp and Abbott*, 1998]. They found that the vertical structure of equatorward currents was consistent with the superposition of the local wind-forced Ekman spiral and the alongshore geostrophic flow due to the set-down at the coast. The poleward flows during relaxations were dynamically consistent with a poleward alongshore pressure gradient force, consistent with other locations off California [*Winant et al.*, 1987; *Lentz*, 1987]. These currents are consistent with the view that upwelled water in the center of the Monterey Bay originates from the north of the bay and not the south.

[6] The anticyclonic California Current (CC) meander, also sometimes referred to as the Monterey Bay Eddy (MBE), is a quasi-permanent feature of the region during

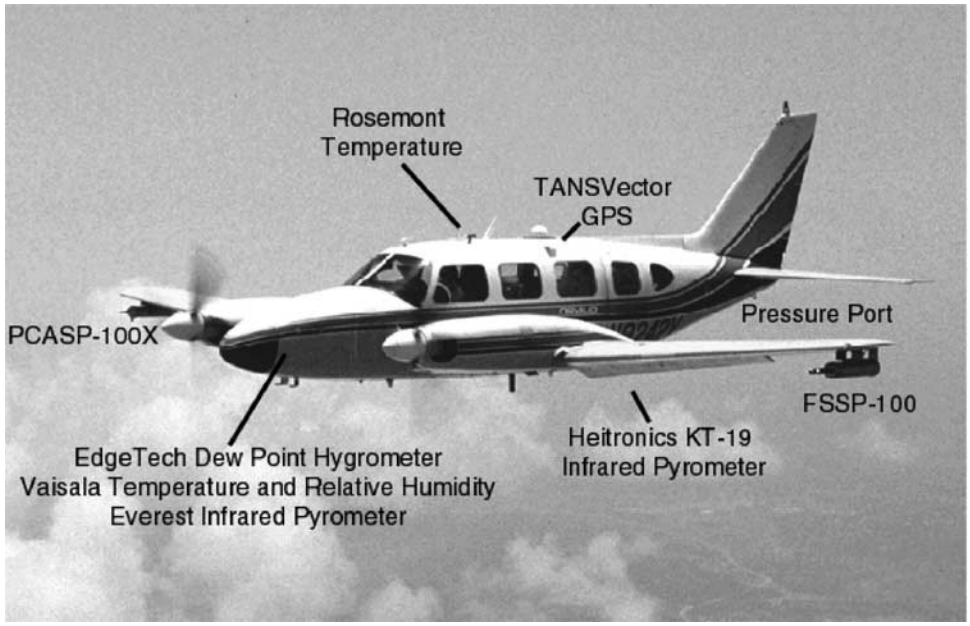

Figure 2. The Navajo aircraft with the positions of the various on-board sensors noted.

the upwelling season [*Rosenfeld et al.*, 1994; *Paduan and Rosenfeld*, 1996]. Drifters suggest that this feature is associated with the larger-scale, meandering California Current System and is not locally generated [*Brink et al.*, 1991]. Moored observations show that the feature is deep, with coherent flows greater than 20 cm s^{-1} exceeding 1000 m depth [*Ramp et al.*, 1997]. The feature is warm and fresh relative to the local waters, displaying the influence of the Pacific Subarctic Water [*Rosenfeld et al.*, 1994]. The MBE is thus an oceanic feature and is clearly not generated by the local wind stress, although it does respond to it. A series of AVHRR images during May and June 1989 showed that the MBE moved rapidly onshore during a wind relaxation event and quickly retreated back offshore when the winds reintensified [*Rosenfeld et al.*, 1994]. Moored observations however have also shown an onshore and southward translation of the MBE without a wind relaxation [*Ramp et al.*, 1997]. The mechanism for this across-shore eddy translation is thus not fully understood.

[7] Intertwined with the upwelling centers and CC meander lies the common thread of the California Undercurrent (CUC). The CUC is observed over the continental slope all along the west coast of the United States [*Pierce et al.*, 2000] and is a ubiquitous feature of all moored data sets both north and south of the Monterey Bay. To the north off the Farallon Islands, the undercurrent was present most of the year but was not coherent with local wind-forcing [*Noble and Ramp*, 2000]. To the south off Point Sur, the currents below 100 m depth are more often poleward than equatorward and frequently exceed 30 cm s^{-1} at 100 m [*Chelton*, 1984; *Wickham et al.*, 1987; *Tisch et al.*, 1992; *Ramp et al.*, 1997]. The poleward flow off Point Sur is pulse-like at very low frequencies (3–4 months) [*Ramp et al.*, 1997]. How this pulse-like flow relates to cross-shore translations of the MBE and potential "blocking" of the flow is of interest but poorly understood. Since Monterey Bay Aquarium Research Institute (MBARI) mooring M2 sometimes samples the CUC, some correlation between the CUC and MBE movements as observed by the aircraft may be possible.

[8] The supertidal (periods shorter than 24 hours) variability in the bay is dominated by semidiurnal tidal currents and locally wind-forced diurnal currents stemming from the sea breeze emanating from the Salinas Valley [*Petruncio*, 1993; *Paduan and Cook*, 1997]. The tidal currents are mostly baroclinic and focus very high energy in the along-canyon component within the MSC [*Petruncio et al.*, 1998, 2002]. The best observations of the supertidal currents over the shallower, continental shelf portions of the bay are from the local HF radar network and indicate semidiurnal current amplitudes of order 20 cm s^{-1} [*Paduan and Cook*, 1997].

[9] The net result of the wind, mesoscale, and tidal forcing within the bay itself is at least two modes of variability. During strong upwelling favorable winds, there is a southward current across the mouth of the bay, northwestward flow on the northern shelf, and eastward flow on the southern shelf resulting in a very well-defined cyclonic circulation in the bay [*Paduan and Rosenfeld*, 1996; *Paduan and Cook*, 1997]. This pattern changes very quickly when the wind stops however, resulting in a confused, less well-defined circulation in the bay [*Paduan and Cook*, 1997]. During this time, the CUC often surfaces [*Tisch et al.*, 1992] resulting in poleward flow off Monterey and colder than usual water in the southern side of the bay. Data revealing the response of the bay to sudden shifts in the atmospheric conditions however are sparse, thus the need for the observational program and results reported here.

3. Data and Methods

3.1. Aircraft Data

[10] The airborne measurements were made using a twin-engine, eight-seat Piper Navajo (Figure 2) owned and operated by Gibbs Flite Center and contracted by SPAWAR

Systems Center San Diego (SSC-SD). During the experiment, the Navajo collected 26 hours of data on 13 flights out of the Marina Airport, Monterey County, California. While the aircraft performed flights for as long as 3 hours, most flights were typically only 110 min long. Each flight for the Navajo consisted of five east/west transects from the coast to 122°30′W plus two more oriented along 315° true north, roughly parallel to the coast north of Santa Cruz (Figure 1). The plane typically flew 130 m above the ocean surface at a true airspeed of ~60 m s^{-1}.

[11] The Navajo carried a NovAtel GPS to provide latitude, longitude, altitude, and vector quantities. A supplemental Trimble TANSVector differential GPS navigational system provided a backup of these quantities as well as aircraft pitch (±0.3°), roll (±0.3°) and azimuth (±0.5°) at 10 Hz temporal resolution. Deconvolution of aircraft true air speed and azimuth from vector speed and direction from the GPS units allowed for the estimation of the wind field. For the flight tracks in this project, wind speed can be estimated to ~1.5 m s^{-1} and direction to ±20°.

[12] State variable instrumentation included a pressure probe, two temperature probes, two dew point/relative humidity probes, and two infrared pyrometers for measuring sea surface temperature. The data were collected at 1 Hz resolution. The static pressure probe was calibrated to ±0.4 mbar accuracy. Through the entire study period temperature values from the Navajo Rosemount and Vaisala probes were within ±0.3°C without correction. The EdgeTech dew point hygrometer (±0.5°C) and Vaisala relative humidity (±5%) probes were within ±0.5°C of dew point. Sea surface temperature was principally measured with a Heitronics KT-19 infrared radiation pyrometer. This instrument measured average SST over a 9.6–11.5 μm wavelength band in a 10 degree angular field of view. This instrument has a 0.1°C precision and a 0.5°C absolute accuracy. A backup Everest 4001 infrared pyrometer probe was also placed in the nose of the aircraft (Figure 2). This instrument has similar wavelength dependencies and a 15 degree field of view. Precision was 0.2°C with an absolute accuracy of 0.75°C.

[13] The sampling strategy was to obtain daily flights during the MBARI Ocean Observing System Upper-Water-Column Science Experiment (MUSE) intensive observation period, with two flights (morning and afternoon) on some days to examine the diurnal variability. The plan was mostly successful except for a 2-day gap during 25–26 August when no pilot was available to fly the plane. All data were downloaded and quality controlled at the NPS Center for Remotely Piloted Aircraft Studies (CIRPAS) at the Marina Airport. The data were moved from there to NPS via the World Wide Web. The data were contoured and overlaid with the buoy and HF radar data at NPS. Maps of the standard parameters were generally available the day after the flight and were made available to the MUSE ships at sea.

3.2. Real-Time Bottom Mounted ADCP Data

[14] Acoustic Doppler current profilers (ADCPs) have become standard technology over the past decade for obtaining vertical profiles of horizontal ocean currents. Recent innovations include trawl-resistant bottom mounts (TRBMs) to protect the instruments from fishing activities, and most recently, acoustic modems to transmit the data to shore in real time. For the MUSE exercise, real-time current profiles were viewed as an asset to help identify the location and vertical extent of the upwelling filaments and fronts. Since an acoustic network was already being deployed to communicate with the autonomous vehicles, an acoustic modem was added to the bottom-mounted ADCP and the instrument was incorporated into the acoustic network. Using this technique, rather than mounting the instrument in a surface buoy looking down, had the further advantage of allowing more rapid sampling (and conversely less averaging) of the ADCP data. This allowed sampling of the internal wave field, which would not otherwise have been possible. The internal waves were thought to be important for mixing over the shelf, with possible direct implications for the distribution of bioluminescence and other biological tracers.

[15] The real-time ADCP was an RD Instruments 300 kHz broadband instrument moored in a TRBM with the transducer heads 0.5 m off the bottom on the 84 m isobath (Figure 1). The instrument sampled in 4-m bins to the surface, however the three uppermost bins within 12 m of the surface were contaminated by surface sidelobe reflection and were not used. The instrument pinged continuously at 2-s intervals and ensemble averages were recorded internally once per minute. At the top of each hour, the most recent ensemble was also transmitted to shore in real time. The acoustic modems used for this purpose were the utility acoustic modems (UAMs) manufactured in-house by the Woods Hole Oceanographic Institution's Acoustic Communications Group. The receiving modem was suspended at 60 m depth from a small, lightweight surface buoy about 300m from the ADCP. This modem was hard-wired to a small controller in the buoy where a handshake was made to a 900 MHz Freewave RF modem for transmission to shore. The shore receiving station was located within line-of-sight at the University of California at Santa Cruz' Long Marine Laboratory. The shore station consisted of a similar modem with 10 dB Yagi directional antenna attached to a PC with an Internet connection. As the packets came in, they were automatically FTP'd to the central "host" PC at MBARI where they were archived and made available to program investigators.

[16] The real-time system performance was excellent. In practice, the receiving end consisted of a network of four buoys and not just one, with the others moored at varying distances away up to a maximum of 10 km from the ADCP. All four buoys were able to transmit error-free data to shore. Several of the surface buoys went down during the experiment but all the ADCP data were transmitted successfully as only one buoy was required, demonstrating the value of acoustic networking. Only one ADCP ensemble per hour was transmitted because the system was being time-shared with other data transmission needs including the AUVs. Each current profile required 12 packets of 50 bytes each for transmission, and took about 5 min to send. With a dedicated system, much higher resolution ADCP data could be moved ashore. Instrument development continues, with the ultimate goal of smaller, lower power systems that could be included into the ADCP housing itself.

3.3. HF Radars

[17] HF radars have been in place in various configurations around the Monterey Bay since 1992. The systems in

place during August 2000 consisted of three CODAR Ocean Sensors Ltd. SeaSonde systems located at Santa Cruz, Moss Landing, and Point Piños, CA. These were single transmit, single receive antenna systems that utilize direction finding (as opposed to beam forming) to localize the return signal [*Barrick et al.*, 1977; *Lipa and Barrick*, 1983]. The Moss Landing antenna operated near 25.4 MHz and the Santa Cruz and Point Piños systems operated near 12.5 MHz. This setup resulted in a radar footprint that included most of the aircraft flight plan (Figure 1).

[18] Only a cursory description of how HF radars sense ocean currents is included here. Some very complete discussions of the basic theory of HF radar operation have now appeared in the literature [*Paduan and Rosenfeld*, 1996; *Paduan and Cook*, 1997] and the reader is referred there for more details. Fundamentally, the operating principle is that radially transmitted incident energy is Bragg scattered back to the receive antenna by surface gravity waves with half the wavelength of the illuminating frequency (5.9 m for the 25.4 MHz wave and 12.0 m for the 12.5 MHz wave). This Bragg peak is much stronger than any of the other returns and stands out above the noise in the return spectrum. Since the surface waves are moving, the frequency of the Bragg peak is Doppler shifted relative to the incident frequency. The shift is due to the wave propagation speed toward or away from the radar plus the velocity of the water itself due to ocean surface currents. The gravity wave speed in deep water however is well known and can be subtracted off to find the speed of the currents. If more than one radar system is deployed it becomes a straightforward geometry problem to translate the radial velocities toward or away from the antennas into the u- and v-velocity components.

[19] The Monterey Bay provides an ideal geometry for deploying these systems. The velocity vectors along the baseline between any two radars (for instance Point Piños and Santa Cruz) are unresolved since the flow toward one is the same as the flow away from the other. The third unit at Moss Landing however resolves this problem since its observations are nearly orthogonal to the baseline. Where good data are available from all three radars, a least squares fit is used to produce the velocity vector for that bin. In practice, the data must be collected over some period of time to produce stable spectral peaks and therefore current velocity estimates. For the systems in use during August 2000, about an hour of averaging was required to produce stable estimates. For the overlays with aircraft SST displayed subsequently, daily-averaged surface velocity vectors were used, which represent very stable and reliable estimates of the subinertial ocean surface currents in the Monterey Bay [*Paduan and Rosenfeld*, 1996].

3.4. Other Data

[20] The primary data sets used in this paper are described above, but several ancillary data sets were also invoked to clarify the analysis. Continuous time series of the surface wind speed and direction were obtained at NOAA buoy 46042, MBARI buoys M2 and M1, and the NPS flux buoy (Figure 1). These data were used to ground truth the aircraft winds and provide the dynamical context for the individual overflights. The M-buoys carried an impressive array of in situ instrumentation as well. Both had a string of twelve SeaBird Electronics Inc. MicroCAT temperature, conductivity, and pressure (TCP) recorders which reported their data in real time using inductive telemetry up the mooring strength member. These instruments spanned the surface to 300 m and sampled at 10 min intervals. Mooring M1 had a downward-looking RD Instruments Inc. 75 KHz broadband "Long Ranger" ADCP. This instrument sampled in sixty 8-m bins using 180 1-s pings every hour, and reliably sampled to 500 m depth. Mooring M2 also had a downward-looking ADCP, a 150 KHz narrowband unit, also from RDI. This unit sampled in 30 8-m bins using 110 1-s pings every 15 min.

[21] The MBARI vertical profiler was moored near the 69 m isobath at 36° 55.3′N, 122°08.4′W, not far from the NPS real-time ADCP (Figure 1). This mooring had a downward-looking RDI 300 KHz workshorse ADCP mounted in the subsurface, taut-moored flotation. The instrument profiled velocity in 4-m bins to the bottom. These velocity profiles are mostly similar to those from the NPS real-time mooring, but differ occasionally as described in the results section.

[22] Finally, there were several research cruises that took place in the Monterey Bay during the MUSE intensive observations period. The CTD data used in this paper were collected from the NEW HORIZON and the RICKETTS.

3.5. Hydrodynamic Model

[23] The ICON model is a thirty-level sigma coordinate model based on the three-dimensional, free-surface version of the Princeton Ocean Model [*Blumberg and Mellor*, 1987]. The model runs on an orthogonal, curvilinear grid [*Shulman et al.*, 2002], which has a variable resolution in the horizontal, ranging from 1.0 to 4.0 km, with finer resolution in and around the Monterey Bay and coarser resolution to the north and south and near the offshore boundary. The model domain extends from just south of Point Piedras Blancas (35.67°N, 121.28°W) in the south to just south of Half Moon Bay (37.48°N, 122.44°W) in the north, extending offshore to 35.60°N, 122.50°W in the southwest and 36.90°N, 123.10°W in the northwest.

[24] The ICON model was forced with 9-km resolution wind stresses and heat fluxes (but not mass fluxes) from the Navy Coupled Ocean and Atmospheric Mesoscale Prediction System (COAMPS™) reanalysis for the U.S. west coast [*Hodur et al.*, 2002; *Kindle et al.*, 2002] and by the Pacific West Coast (PWC) model [*Haidvogel et al.*, 2000; *Rochford and Shulman*, 2000] on the seaward boundaries. This was a one-way nesting scheme, i.e., the PWC forced the ICON model boundaries but not vice versa. The PWC extends seaward to 135°W longitude and from 30°N to 49°N latitude. The PWC model assimilated the space-based Multichannel Sea Surface Temperature (MCSST) data, and was forced using the 27-km winds from COAMPS™ and fields from the operational Navy Layered Ocean Model (NLOM) [*Rhodes et al.*, 2001] at the open boundaries. The ICON model also assimilated surface currents from the HF radars around the Monterey Bay using a combination of the physical-space statistical analysis system (PSAS) at the surface and Ekman projection of the surface corrections into the interior [*Shulman et al.*, 2001; *Paduan and Shulman*, 2004].

[25] This paper takes advantage of the continuous series of maps of the bay which show the space and timescales over which the circulation developed, and the transitions

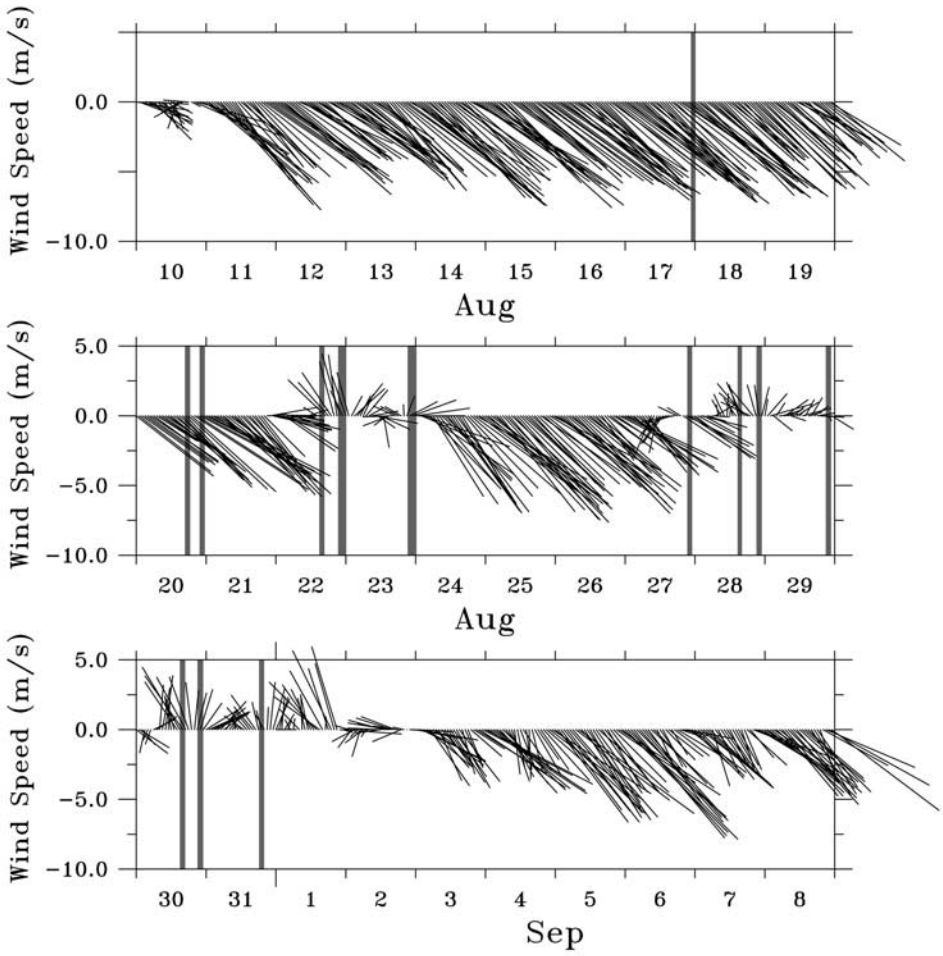

Figure 3. Wind speed and direction from 10 August to 8 September from NOAA buoy 46042 located just off the mouth of the Monterey Bay (see location in Figure 1). The length of the lines indicates the wind speed and the orientation indicates the direction the wind is blowing toward (oceanographic convention). The shaded lines indicate the times when the aircraft overflights were performed.

between upwelling and downwelling favorable winds. The aircraft meteorological maps reveal previously unsampled submesoscale atmospheric features, and with the HF radar and SST maps, show the impact of these features on the ocean circulation beneath them. The moorings show the vertical extent of the surface features that help us to understand their dynamics and the transitions between the upwelling and relaxation states. The ICON model assimilates the surface velocity data and extends the value of the observations into the ocean's interior. It also includes important variables such as salinity that were not sampled by the aircraft, radars, or ADCPs.

4. Results

[26] The wind velocity vector plots from NOAA buoy 46042 with the overflight times indicated by the vertical gray bars (Figure 3) provide the context for discussing these results. Prior to the first flight on 17 August, the winds were upwelling favorable at 10 m s^{-1} for 6 days starting on 11 August 2000. This was followed by a brief relaxation event that lasted only about a day-and-a-half from noon on the 22 through 23 August. The northwest winds resumed at about the same speed, 10 m s^{-1}, during 24–26 August and part of the 27 August. The remainder of the flights occurred during an extended wind relaxation event from 28 August through 2 September, which included two exceptionally calm days on 30–31 August. A central result of this study is how the Año Nuevo upwelling center and the MBE respond to the upwelling versus relaxation wind regimes. Thus this section is organized around reporting the conditions during the first upwelling, brief relaxation, second upwelling, and extended relaxation events.

4.1. Conditions During the First Upwelling Event

[27] The 17 and 20 August flights took place during strongly upwelling favorable conditions (Figure 4). Both days showed a distinct, cold upwelling filament extending south-southeastward off Point Año Nuevo with minimum temperatures less than 11°C. The filament was very well defined on 17 August but had advected over the MSC by 20 August. This notion is supported by the HF radar vectors that showed a coherent southward jet across the mouth of the bay on 17 August but onshore currents during 20 August. The jet held the cold water offshore on 17 August until it broke down sometime between

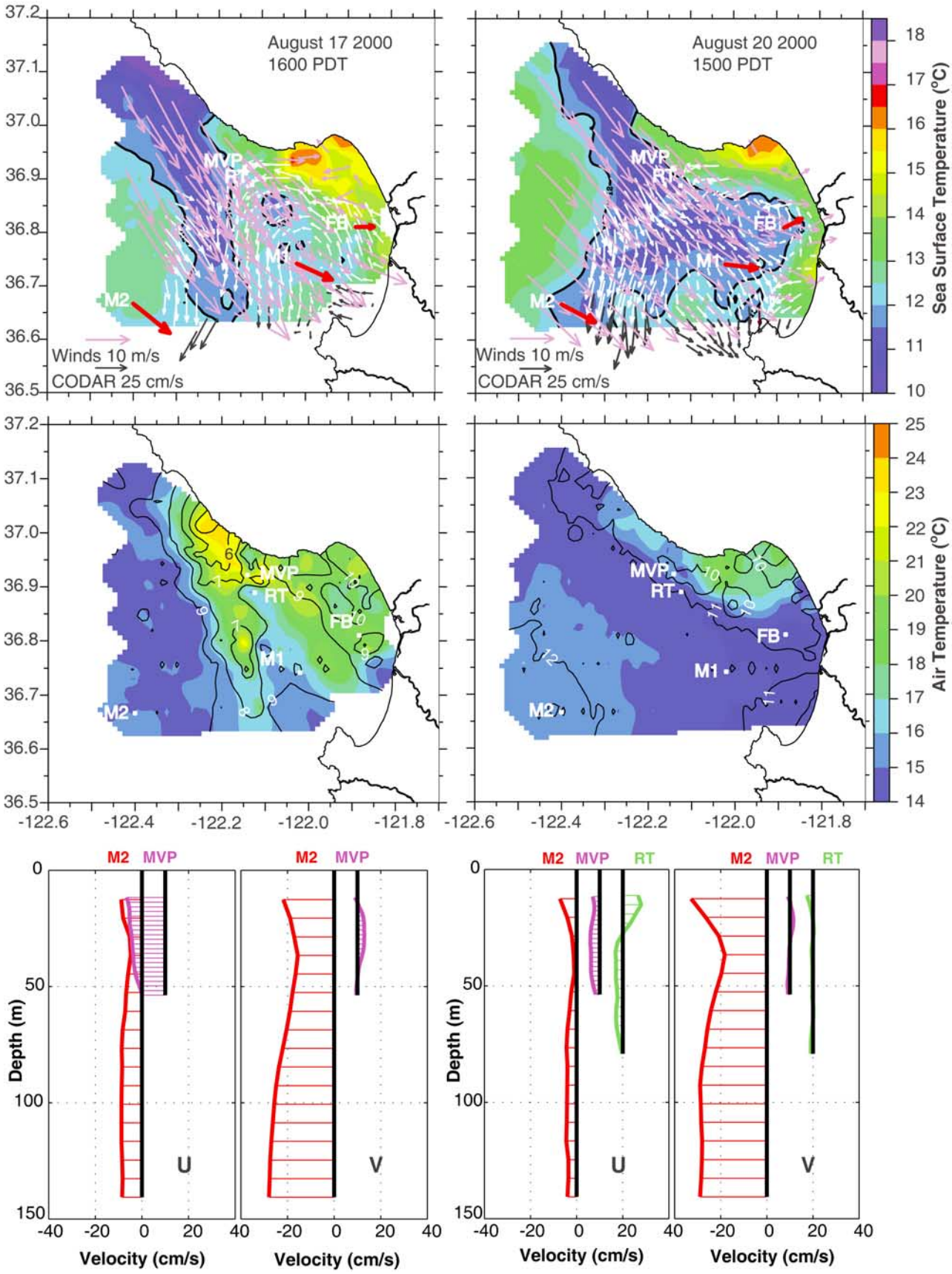
August 17 2000
1600 PDT
August 20 2000
1500 PDT
MVP
RT
FB
M1
M2
Winds 10 m/s
CODAR 25 cm/s
Sea Surface Temperature (°C)
Air Temperature (°C)
Depth (m)
Velocity (cm/s)
U
V

Figure 4

17 and 20 August. This advection of cold water from the north over the center of the MSC is consistent with the earlier hypothesis [*Rosenfeld et al.*, 1994] that advection rather than local upwelling in the canyon is the source of the cold surface water often observed in the center of the bay.

[28] The SST maps also show a warm (>16°C) patch in the northernmost corner of the bay. This feature is commonly attributed to "wind shadowing" by the Santa Cruz mountains that protect this area from the prevailing northwesterly winds offshore [*Graham*, 1993; *Graham and Largier*, 1997]. These data verify this hypothesis conclusively for the first time, as the aircraft wind vectors observed over the warm patch were weak and confused when compared to the strong coherent flows further offshore (Figure 4, top). This allows for a shallower surface mixed layer, greater local heating due to solar insolation, and higher SST in the warm patch than in other parts of the Monterey Bay.

[29] The aircraft winds showed a southeastward jet directly over the cold filament on 17 August and a broader, more uniform, slightly more onshore wind field on 20 August. These onshore winds are consistent with the CODAR surface current vectors and no doubt contributed to advecting the cold water into the bay. Of particular interest are the air and dew point temperatures (Figure 4, middle) observed by the aircraft on 17 August, which showed a hot, dry atmospheric jet directly over the cold filament in the ocean, with comparable scales. This jet seems to have originated in the Santa Cruz mountains on the north side of the bay. Atmospheric features of this scale have not been previously observed over cold coastal filaments, and may play an important role in the ocean dynamics. By the time of the 20 August survey, the air temperature pattern did not show this atmospheric jet, and instead more generally reflected the SST pattern.

[30] The current profiles (Figure 4, bottom) show nearly barotropic southwestward flow over the entire upper 240 m at M2 for both days, consistent with the mooring's position with respect to the MBE. The MBE was weak in these presentations, located mostly offshore of this view. The flow at MVP was west-northwestward over the continental shelf on both days, albeit weaker on 20 August. The RT mooring was not yet deployed on 17 August, but on 20 August showed southeast flow over the upper 30 m and northwest flow below. The MVP and RT moorings were not far apart, but the SST maps indicate MVP in the warm water (or perhaps the front between the warm and cold water) moving WNW out of the bay around the corner past Año Nuevo, while RT was in the wind-driven cold filament. The profile shape at RT was consistent with those observed at similar depths on the continental shelf off Point Sur [*Ramp and Abbott*, 1998] during upwelling events and indicate an Ekman depth of about 30 m.

4.2. Conditions During the Brief Relaxation

[31] Three flights captured the ocean variability during the short relaxation event of 22–23 August: These flights took place at 0800 22 August, 1500 22 August, and 1400 23 August. While most flights were scheduled in the afternoon to avoid morning fog in the bay, conditions were favorable for a morning flight on 22 August, and the contrasts between the morning and afternoon flights are remarkable over just 7 hours time (Figure 5). In the morning (Figure 5, top), the size of the upwelling center off Año Nuevo was much reduced with respect to August 20 (Figure 4) and most of the bay had warmed about 1°C to between 12°–13°C. By afternoon (Figure 5, middle), the bay had warmed another 1°C under the prevailing southwesterly winds. The warming was slightly greater off Santa Cruz (about 2°C to >16.5°C) likely preconditioned by a shallower mixed layer there. All this warming can be ascribed to local surface heating rather than advection as the CODAR vectors indicated very weak surface currents over most of the bay. The only exception was a well-defined onshore jet heading toward Point Piños in the southern side of the bay, well away from the regions where the greatest SST changes took place. Comparing the wind vector maps for 0800 and 1500 shows the diurnal sea-breeze dramatically: There was almost zero wind at the head of the bay near Moss Landing in the morning, rising to order 10 m s^{-1} onshore in the afternoon. This was true of all occasions when two flights were made during the same day (20, 22, 28, and 30 August, not shown).

[32] A day later on 23 August, the upwelling center off Año Nuevo had completely disappeared, but interestingly, the SST within the bay proper had decreased by order 0.5° to 1.0°C. This is counter-intuitive, and the surface waters in the bay generally warm during a wind relaxation event. This cooling phenomenon appears to be due to submesoscale spatial variability in the surface wind stress. The winds along the north coast of the bay were quite different from the winds observed at buoy M2. The buoy winds (Figure 3) showed the large-scale relaxation typical of the entire central coast, but a strong, coherent, southeastward jet was blowing at 8–10 m s^{-1} into the bay along the Santa Cruz coast (Figure 5, bottom). This jet linked up with the afternoon sea breeze and continued into the Salinas Valley. This wind jet, apparently the result of local processes which are not well understood, induced sufficient mixing in the ocean beneath it to slightly lower the SST.

[33] The strong near-surface stratification during the early morning hours on August 23 is shown by the CTD section taken from the R/V *Ricketts* across the continental shelf on

Figure 4. Aircraft and mooring data from 17 (left panels) and 20 (right panels) August during the first upwelling favorable wind stress event. The top panel shows the aircraft (100 m) winds (magenta vectors) and CODAR surface currents (white vectors) overlaid on sea surface temperature (color contours). The surface winds from the MBARI M-buoys are included as red vectors for comparison. The middle panel shows the 100 m air temperature (color) and dew point temperature (black contours) as observed by the aircraft. The bottom panel shows the daily-averaged current profiles as observed at buoys M2 (orange), MVP (magenta), and RT (green). In all cases, currents to the right of the vertical black (zero) line are positive (east, north) and to the left are negative (west, south). All the profiles are scaled according to the abscissa, and the origins have been offset for clarity.

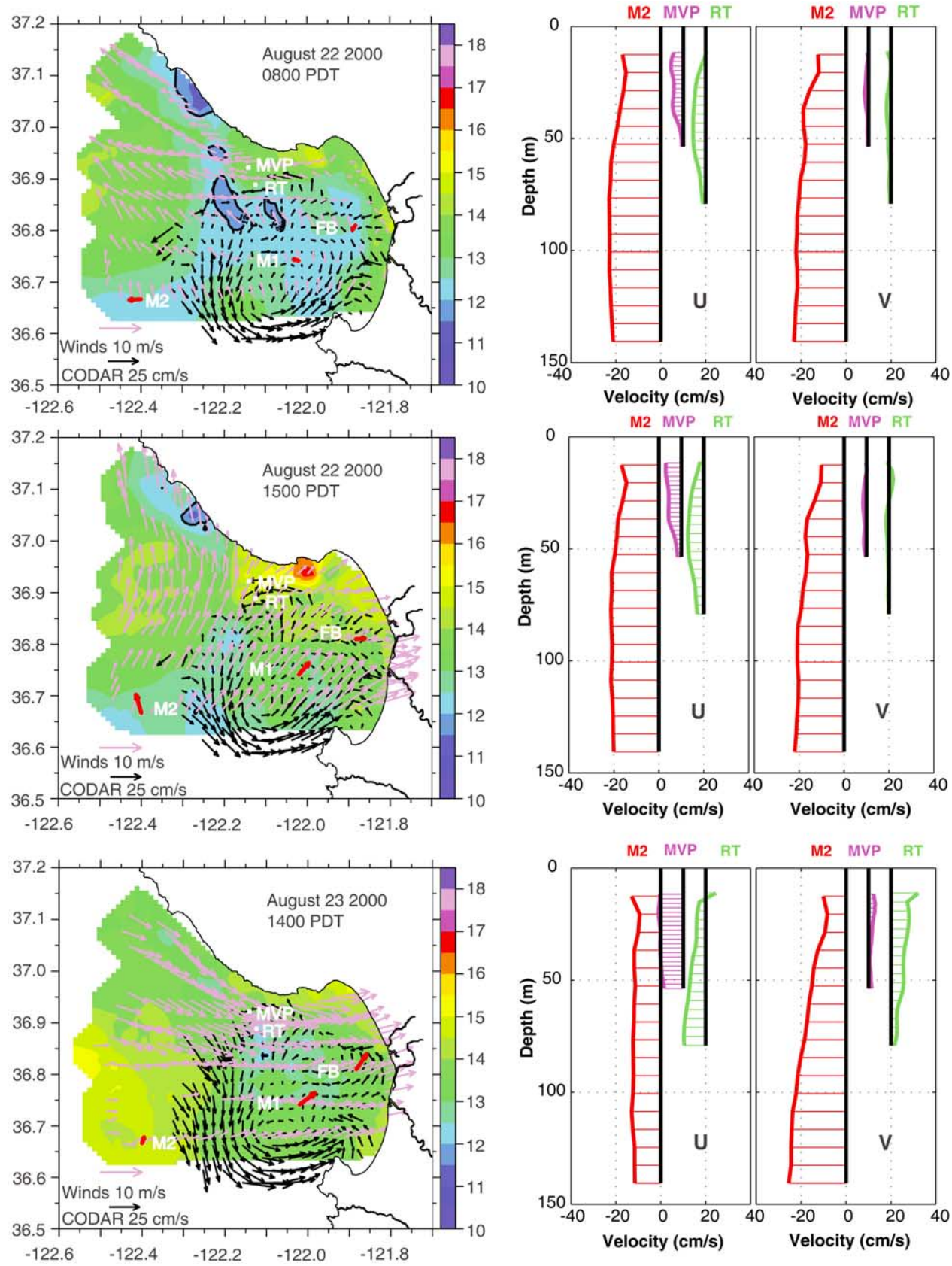

Figure 5. Aerial maps and current profiles from 0800 22 August (top), 1500 22 August (middle), and 1400 23 August (bottom). The left- and right-hand panels are the same as the top and bottom panels in Figure 4 respectively, except the CODAR vectors are now in black for better clarity.

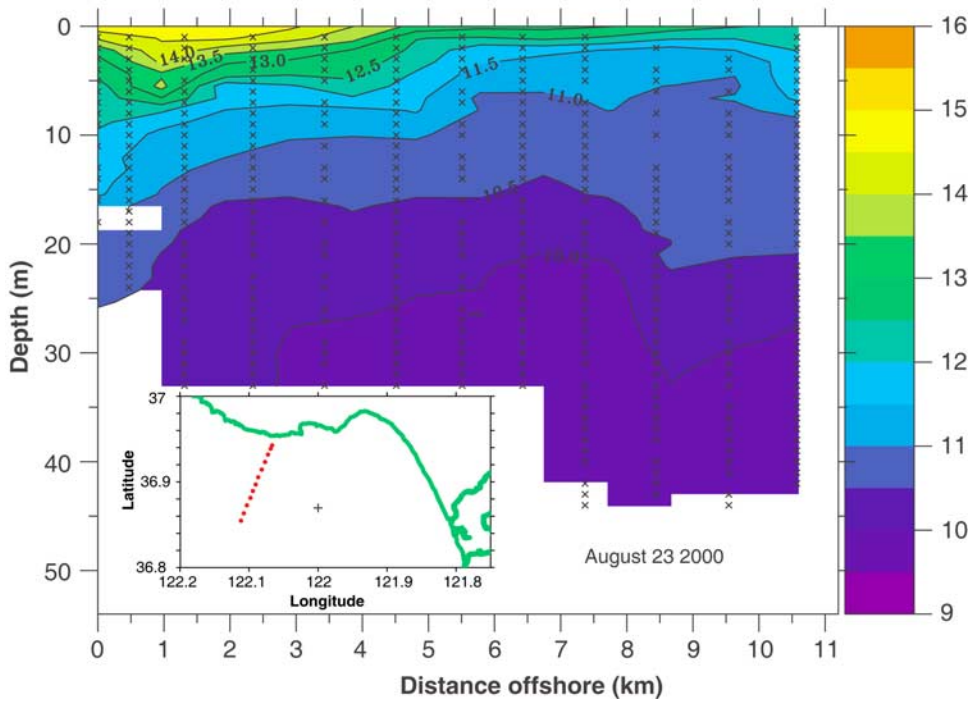

Figure 6. Temperature transect off Santa Cruz, California, collected from the R/V *Ricketts* during the early morning hours of 23 August 2000. Note the very shallow stratified layer that existed in the upper 5 m of the water column. The inset shows the transect location in the northern part of the Monterey Bay. The cross indicates the location of the CTD profiles shown in Figure 7.

the northern side of the bay (Figure 6). This transect shows that away from the coast, the temperature increased from 11.5° to 13.0°C in the upper 5 m of the water column. The surface cooling as the day went along is shown by a time series three CTD stations taken by the R/V *New Horizon* (Figure 7), located not far from the transect (see locator map in Figure 6). The early casts (stations 13 and 14) show the strongly stratified near surface layer with temperatures consistent with the RICKETTS section. After the wind kicked up, the 1130 LT cast shows the cooling of the surface water from >12.5°C to about 12.0°C. Thus these submesoscale wind jets have significant impacts on the conditions within the bay, and more research is needed to understand the physics underlying these events.

[34] Currents in the water column (Figure 5, right half) near M2 were still southward, but much more westward than during the upwelling event. This seems due to the mooring's position on the SE side of the clockwise (anti-cyclonic) MBE as it translated onshore during the brief relaxation event. Currents on the shelf (RT and MVP) were more northwestward and less vertically sheared, exiting the bay. These are consistent with the CODAR patterns that showed a counter-clockwise circulation in the bay during this time.

4.3. Conditions During the Second Upwelling Event

[35] Winds during the second upwelling event during 24–27 August had magnitudes similar to the first event (order 10 m s^{-1}) but lasted only three days rather than ten. This event was unfortunately not sampled by the aircraft as the next flight was not until 1400 on 27 August, just after the event ended. A partially clear satellite image on 24 August (not shown) showed a hint of upwelling just starting off Año Nuevo. Surface currents within the bay persisted in their counterclockwise sense, quite similar to the pattern at 1400 on 23 August (Figure 5). The current profiles on 24 August were similar to those on 20 August (Figure 4, bottom) under similar wind conditions. Currents on the shelf (MVP) were WNW while currents just slightly offshore (RT) followed the wind-forcing in the surface Ekman layer and continued WNW below.

4.4. Conditions During the Extended Wind Relaxation Event

[36] The final seven flights, two in the morning and five in the afternoon, were executed daily from 27 to 31 August during an extended wind relaxation event. These data undoubtedly provide the best documentation to date of the bay's response to these conditions. Viewed collectively, the most striking aspect of the temperature maps (Figure 8) is the onshore translation of the MBE as suggested by previous authors [*Rosenfeld et al.*, 1994]. On 27 August (Figure 8a), the wind vectors were just starting to reverse so this map represents the initial conditions for the onshore translation event. This map is strikingly similar to the 23 August map, with a southeastward and onshore wind jet persisting along the northern coast of the bay even as the winds generally weakened. The MBE was centered near 36.9°N, 122.5°W with maximum SST between 15.5° and 16.0°C. Translation of the eddy center is difficult to track, as the center was not well defined and may in fact lie beyond the field of view in these maps. The maximum SSTs

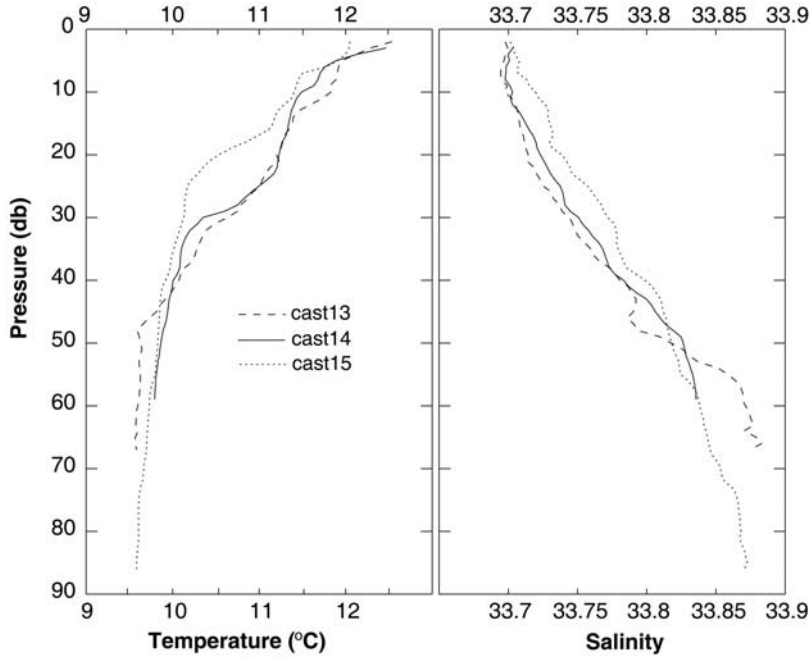

Figure 7. A time series of CTD profiles collected from the R/V *New Horizon* on 23 August 2000. All were collected very near 36.87°N, 122.00°W. The dashed, solid, and dotted lines were collected at 0100, 1000, and 1130 LT, respectively.

observed in the eddy between 27 and 31 August were 15.5°, 16.0°, 17.5°, 16.5°, and 16.5°C respectively. The positions of these maxima (Figure 8) qualitatively suggest southward and onshore translation of the MBE during this time.

[37] The front separating the MBE and the ambient bay water, centered around T = 14.0°–14.5°C (light green to yellow in the figures) can be followed more quantitatively. The maximum eastward position of this front on 27 August was along 122.35°W. From 27 to 28 August, this front moved eastward to 122.30°W. Between 28 and 29 August, the front did not translate further eastward, but it broadened and expanded southward, covering much more of the mouth of the bay. This was also consistent with a southward translation of the eddy center. By 30 August, the front had moved slightly eastward to 122.25°W. These data collectively suggest eastward translation of the front about 0.05 degrees of longitude per day, equivalent to about at speed of 5 km d^{-1} at this latitude.

[38] On 31 August, temperatures within the bay itself were so high that the eddy front could no longer be located unambiguously. This was an unusually calm day, and two temperature maxima were present, one in the MBE and a second, 0.5°C warmer one in the center of the bay itself (Figure 8, center right panel). The offshore maximum is ascribed to a combination of advection and surface heating, but primarily advection, while the inner bay thermal maximum was due to surface heating. This can be readily seen in the time series plots for buoys M1 and M2 (Figure 9). The plot for buoy M2 (bottom panels) shows a warm (T > 16.5°C), fresh (S < 33.3 psu) feature, strong in the upper 40 m but still visible at 100 m, slowly moving into the area. The low salinities are indicative of offshore Pacific Subarctic Waters and the temperatures are consistent with those observed by the aircraft. The warmest temperatures at buoy M1 on the other hand (top panels) were only about 14.5°C versus >17.5°C observed by the aircraft, indicating that the warming in the center of the bay was a skin effect on an unusually calm day. While such conditions are unusual along the California coast in summer they are not unprecedented: Temperature changes exceeding 4°C in the upper 2 m have been previously observed off Point Arena [*Ramp et al.*, 1991], also on a flat-calm day.

[39] The CODAR vectors in this sequence consistently show northeastward flow into the bay from the south around Point Piños. There was also a southwestward flow along the SE quadrant of the MBE consistent with the eddy's anticyclonic circulation. Unlike earlier scenes, there was no westward flow connecting the two. The flow around Point Piños seemed to originate from the south rather than offshore. The WNW surface flow off Santa Cruz was still present but weakened slightly on 31 August. The flow in the central part of the bay was weak.

[40] The current profiles could be summarized by the profiles from 28 and 31 August (Figure 10). The 28 August profile was representative of 27–30 August when the profiles were nearly identical. This was the "usual" condition with barotropic WNW flow over the northern continental shelf and SW flow over the entire upper 350 m at buoy M2. The 31 August profile was the only one observed where the flow at M2 turned toward the southeast. This occurred only during the time when the MBE was at its maximum east- and southward position.

4.5. Model Predictions During Upwelling and Relaxation Events

[41] The ICON model predictions computed using a variety of forcing and data assimilation schemes have been rigorously compared to in situ observations in the Monterey

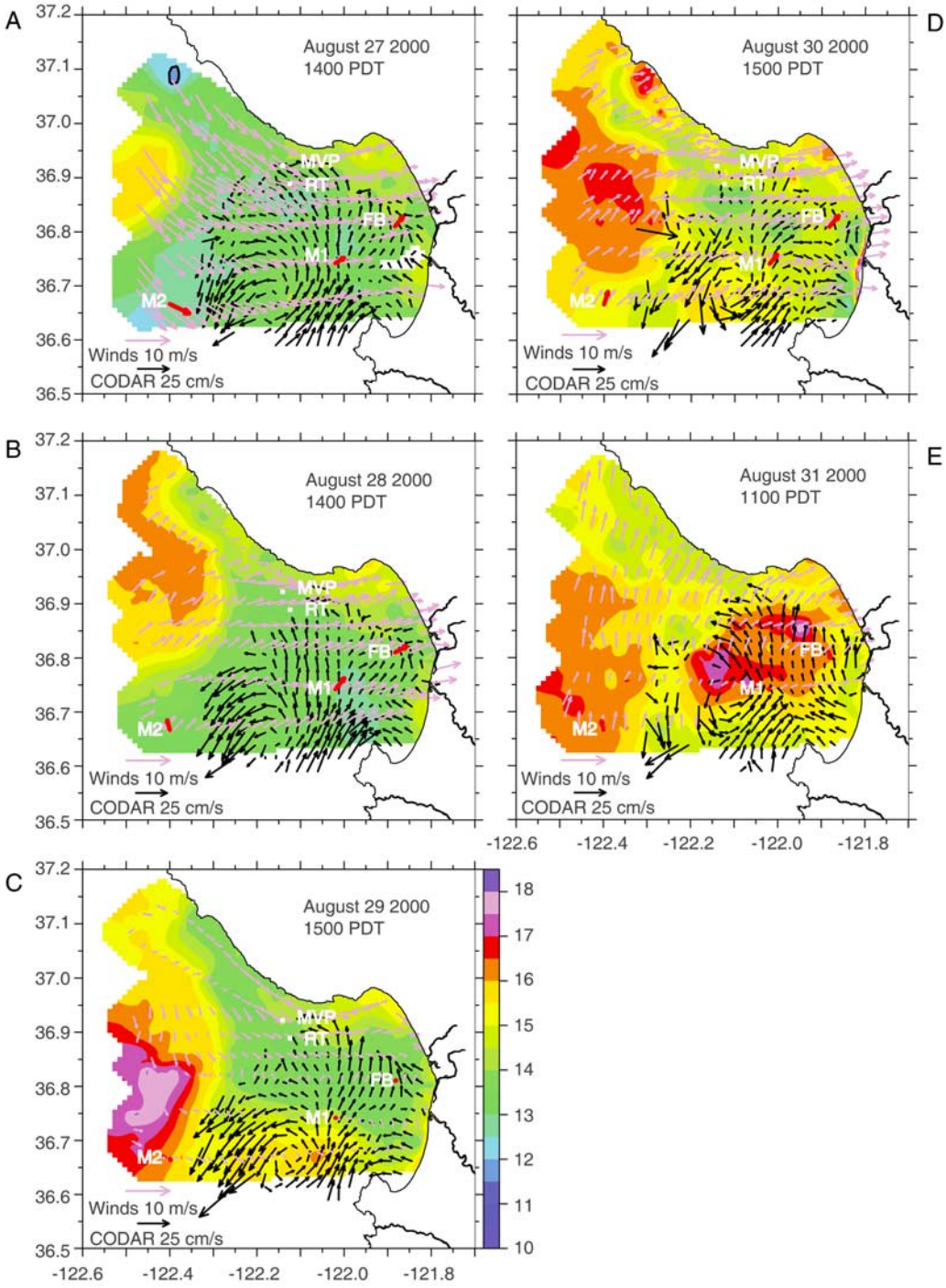

Figure 8. A time series of maps constructed from aircraft and in situ data during an extended wind relaxation event over the Monterey Bay. Each panel shows the aircraft (100 m) winds (magenta vectors) and CODAR surface currents (black vectors) overlaid on sea surface temperature (color contours). The surface winds from the MBARI M-buoys are included as red vectors for comparison. The maps are from (a) 1400 on 27 August 2000, (b) 1400 on 28 August 2000, (c) 1500 on 29 August 2000, (d) 1500 on 30 August 2000, and (e) 1100 on 31 August 2000.

Bay [*Shulman et al.*, 2002; *Paduan and Shulman*, 2004] using complex correlation analysis [*Kundu*, 1976]. It was demonstrated that assimilation of CODAR-derived surface currents significantly improved the ICON model predictions [*Paduan and Shulman*, 2004]. Similar comparisons were made for the August–September 2000 time period discussed here using the optimal assimilation schemes and Ekman projection depth (46 m) determined by the earlier

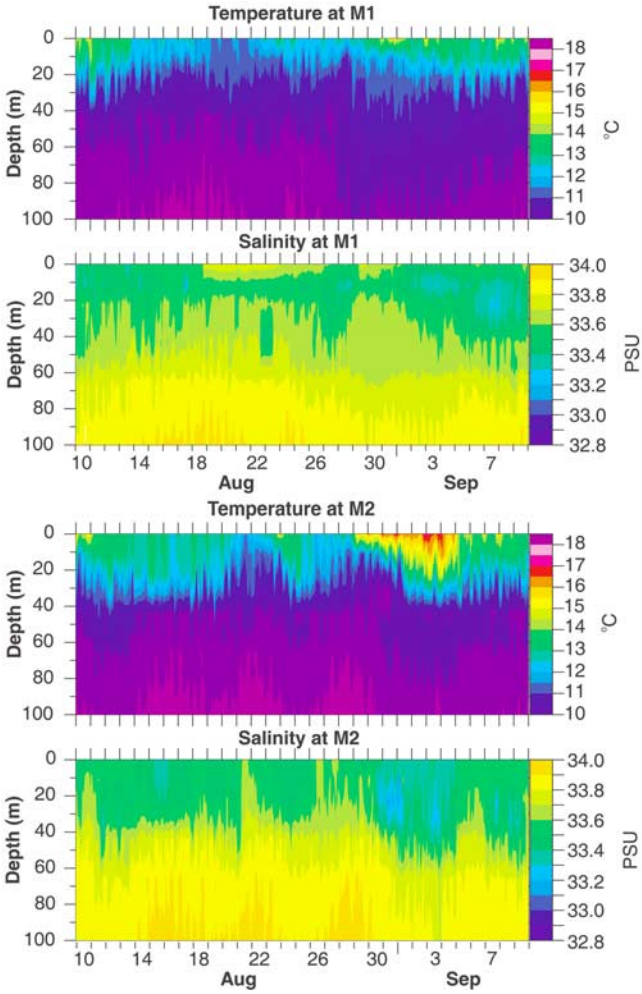

Figure 9. Time series of upper-ocean temperature and salinity from buoy M1 (top) and M2 (bottom) during August and September 2000. The buoy locations are as shown in Figure 1.

experiments [*Paduan and Shulman*, 2004]. Magnitudes of complex correlations between model-predicted and observed currents were significantly correlated between the surface and 100 m for both buoys M1 and M2 (Figure 11). The direction of the current was very good at M1 (near zero deviation between 30 and 70 m) and less than 20 degrees deviation over the upper one hundred meters at M2 (Figure 11). These results indicate good agreement between observations and model predictions for the average magnitude and direction of the currents.

[42] Also of interest are comparisons between the observed and model generated temperatures and salinities. Root mean square (RMS) errors, expressed as a percentage, in predicted versus observed temperature and salinity at moorings M1 and M2 were estimated as

$$RMS = \frac{\left(\sum_t (f^m - f^o)^2\right)^{1/2}}{\left(\sum_t (f^o)^2\right)^{1/2}} \times 100$$

where f^m and f^o are model-predicted and observed temperature (salinity) respectively. Overall, the RMS error was less than 1% for salinity and less than 16% for temperature (Table 1). These are likely worst-case errors, since there are often spatial and temporal shifts between model predicted and observed mesoscale features [*Paduan and Shulman*, 2004]. As a result, relatively small spatial offsets in the modeled features can lead to an unrealistically poor assessment of the model predictions when comparisons are done with single-point moored observations.

[43] The surface temperature and velocity vectors were generated for the MUSE time period using the ICON model as described in the data and methods section. The model results were plotted using the same spatial scales and color bars as the observations to facilitate direct comparisons between the two in terms of the absolute values and feature patterns represented. The model output also provides a continuous time series from which to study the temporal evolution of events and the transitions between them, including during the times when the aircraft did not fly.

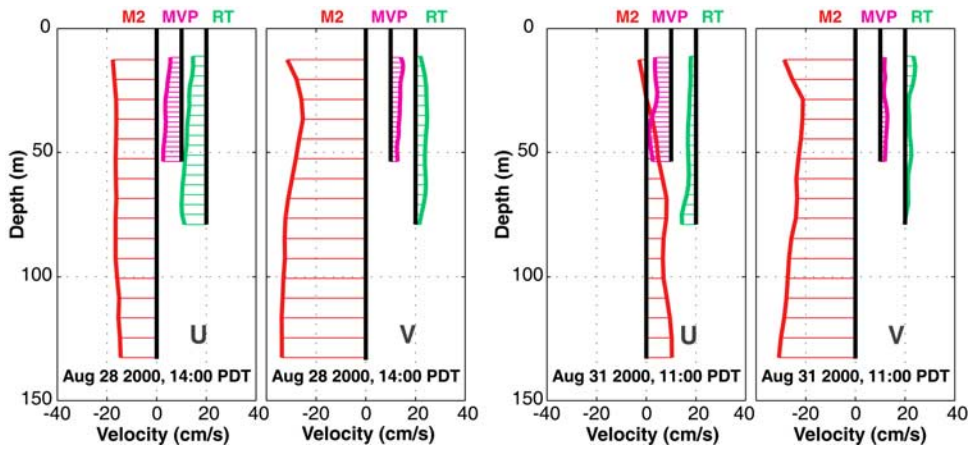

Figure 10. Daily-averaged current profiles as observed at buoys M2 (orange), MVP (magenta), and RT (green) for 28 August 2000 (left panel) and 31 August 2000 (right panel). Currents to the right of the vertical black (zero) line are positive (east, north) and to the left are negative (west, south). All the profiles are scaled according to the abscissa, and the origins have been offset for clarity.

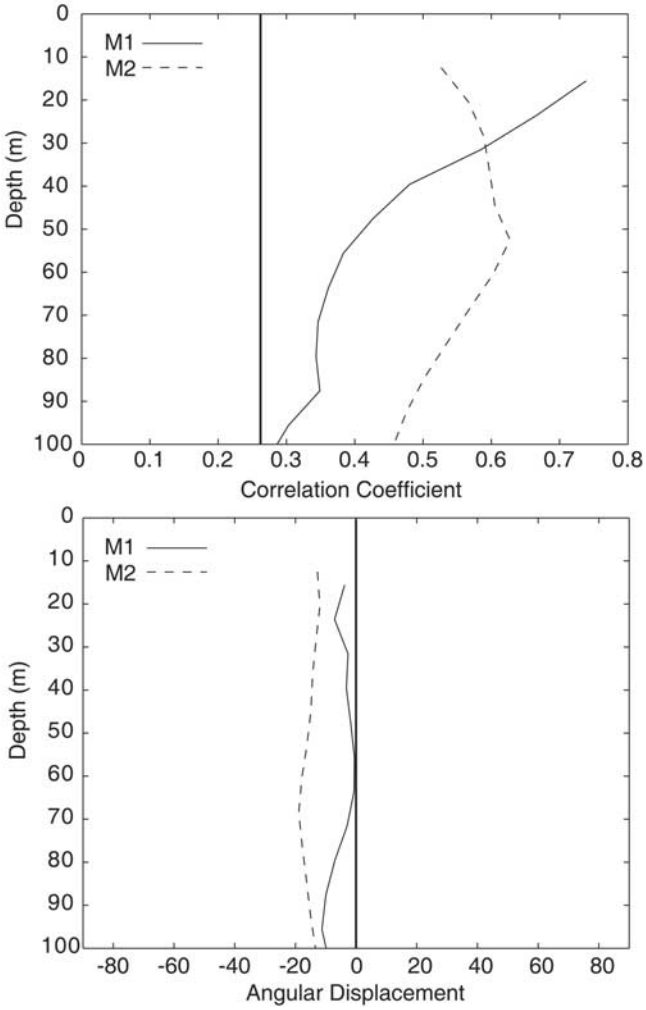

Figure 11. The magnitude of the complex correlation coefficient (top) and angular displacement of direction (bottom) as a function of depth between the ICON model generated and observed currents at buoy M1 (solid line) and M2 (dashed line) during August 2000 in the Monterey Bay. The angle gives the average counterclockwise rotation of the model currents with respect to the buoy (ADCP) currents. The solid vertical line indicates the significance level [*Emery and Thomson*, 1998] for correlation at the 95% level (0.261).

[44] No sea surface temperature data from satellites or aircraft were assimilated in these ICON model runs. The CODAR HF radar vectors were assimilated where available under the radar footprint (Figure 1). Thus some of the current vectors such as within the Monterey Bay were necessarily similar between the model and observations, but the effect of this assimilation on the surface velocity vectors outside the radar footprint was yet to be determined. Model/data comparisons at buoy M2, which was outside the radar footprint, were dramatically improved by assimilating the surface velocities [*Paduan and Shulman*, 2004]. The ICON model domain was larger than the aircraft flight track but smaller than the mesoscale features of the offshore California Current System. In some cases, the sources of the model variability were readily apparent, and in other cases less so. The issues of water mass structure and remote forcing along the coast from outside the ICON model domain are taken up subsequently in the discussion section.

[45] During the first upwelling event (17–20 August) the model predictions were very consistent with the observed upwelling dynamics and supported the hypothesis that the upwelled water from near Point Año Nuevo was advected into the Monterey Bay over these four days (Figure 12). The velocity vectors show the development of a southward jet, persistent over all 4 days, and the development of a cyclonic circulation within the bay. There is some evidence of horizontal mixing across the mouth of the bay where the cold upwelled water flows southward next to the warmer water within the bay. The model current vectors at 50 m depth (not shown) indicate that this basic circulation pattern persisted to that depth over the southern and northern continental shelves within the bay. On 19 and 20 August (Figure 12c) the cold plume stemming from Año Nuevo extended fully across the mouth of the bay and effectively blocked the warmer (and less saline) offshore water from entering the bay. South of the bay, the larger domain of the model (not shown) indicates the development and offshore movement of a second cold filament from the upwelling center off Point Sur [*Breaker and Mooers*, 1986; *Tisch et al.*, 1992; *Rosenfeld et al.*, 1994; *Ramp et al.*, 1997]. This offshore flow may result from the convergence of the southward jet originating off Año Nuevo and the poleward flow along the coast south of Point Sur.

[46] The ICON model faithfully reproduced the warming over the central and offshore portion of the bay and the onshore surface flow near Point Piños during the 22–23 August relaxation event (Figure 12d). The equatorward jet offshore was completely masked by surface heating. The model currents along the coast within the bay itself were much less organized than during upwelling favorable winds, possibly due to the short duration of the relaxation event. They were mostly directed onshore however, consistent with the Ekman transport and the poleward wind stress. The small cyclonic gyre centered near 36.65°N, 122.10°W with associated onshore flow near Point Piños resulted from the convergence of poleward flow along the Point Sur coast with equatorward flow to the north. The model was not able to produce the cooling in the bay as observed on 23 August. This was likely because the submesoscale jet off Santa Cruz

Table 1. Percent Root Mean Square Error Between Observed and ICON Model-Predicted Temperature and Salinity Values at Selected Depths on Moorings M1 and M2 in the Monterey Bay[a]

	M1		M2	
Depth, m	% RMS Salinity	% RMS Temperature	% RMS Salinity	% RMS Temperature
0	0.46	9.3	0.61	7.9
10	0.45	11.0	0.61	6.1
20	0.37	15.6	0.55	7.1
30	0.37	14.4	0.59	7.7
40	0.37	14.0	0.65	9.2
50	0.39	10.4	0.65	6.7
60	0.4	8.9	0.64	6.4
70	0.37	7.1	0.58	5.3
80	0.35	5.8	0.55	4.7
90	0.3	4.9	0.47	4.0
100	0.25	4.2	0.38	3.7

[a]RMS, root mean square.

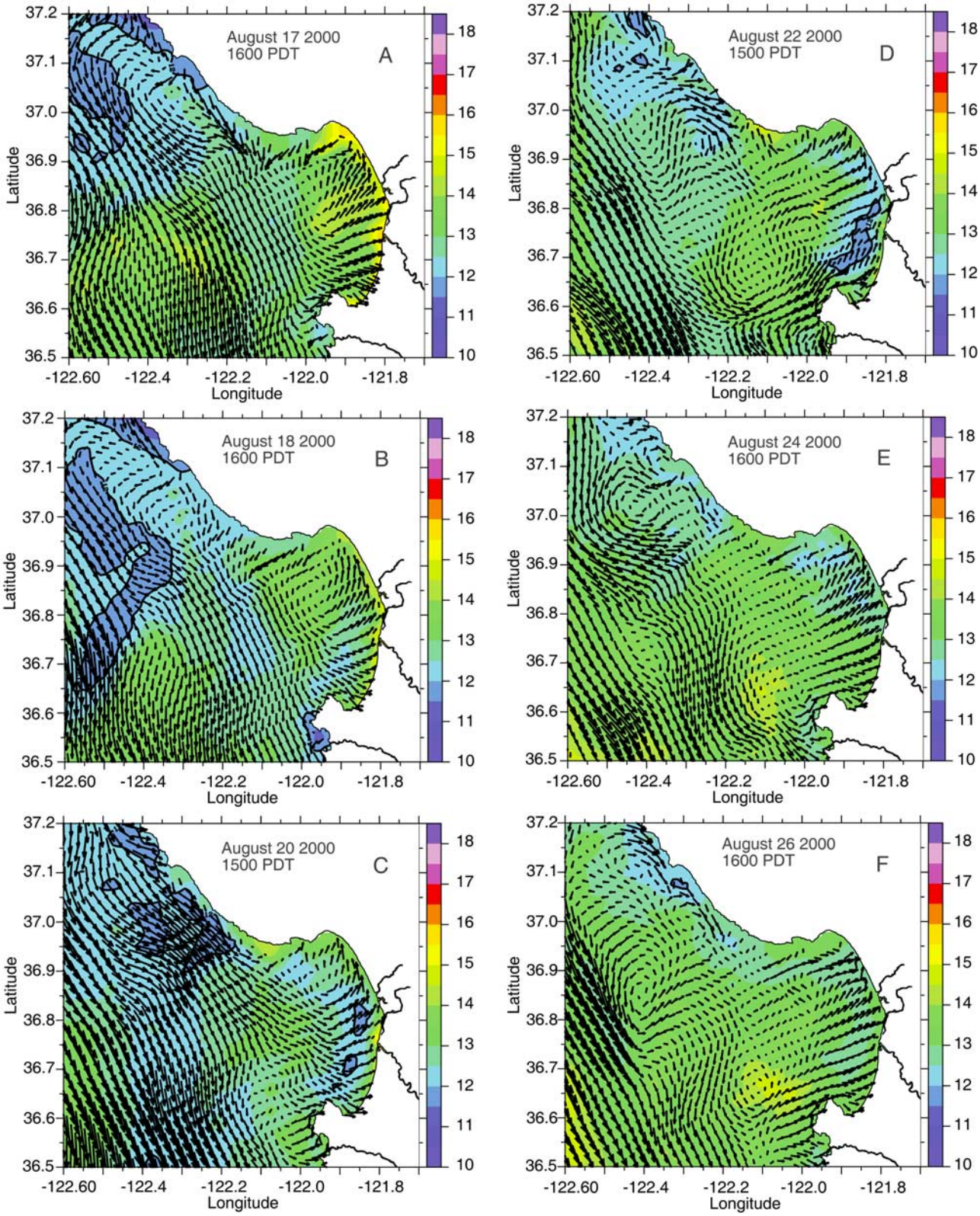

Figure 12. Surface currents and sea surface temperature from the ICON model on 17, 18, 20, 22, 24, and 26 August 2000. The scales are the same as those used for the observations in Figures 4, 5, and 8.

was not well represented in the 9 km COAMPS™ winds used to force the model. Thus the observed breakdown of the near-surface stratification (Figures 6 and 7) did not occur in the model output. The fine-scale physics of the very near surface was not well represented in the model, which was designed primarily to study the mesoscale ocean features.

[47] The model output during the second, short upwelling event provides valuable insight in the continuity of events during the absence of aircraft data. The model SST showed very little change during the 24–26 August time frame (Figures 12e and 12f). There was a slight expansion of the cold water off Point Año Nuevo on 24–25 August in keeping with the 24 August satellite image, but no cold southward jet appeared. Comparing the 11–20 August and 24–26 August wind events suggests that on the order of a week of sustained upwelling favorable winds is required for the cold southward jet to form.

[48] During the final extended relaxation event, the ICON model also showed the warm water in the MBE advecting onshore over time, but the warm feature remained farther offshore than in the observations (Figure 13). The model was not able to reproduce the extraordinary surface heating within the bay during 30–31 August. As discussed earlier, this was likely due to inadequate forcing of both the wind stress and the surface heat fluxes from the 9-km COAMPS model and insufficient structure in the extinction coefficients in the model upper ocean, which is necessary to trap incoming solar radiation in a surface microlayer [*Ramp et al.*, 1991]. Despite this shortcoming, the model remained effective at reproducing the observed ocean currents. The equatorward flow along the inshore side of the MBE, the poleward flow around Point Piños into the bay, and the development of a cyclonic eddy off Point Piños between these two opposing flows were all present in both the observed and computed currents. The eddy position, centered near 36.65°N, 122.15°W, was similar to its position during the previous (22–23 August) wind relaxation event. The circulation in the bay itself was cyclonic, but brought different water masses into the bay: During upwelling events the entering water came from the north and/or offshore, while during the relaxation events the water came from the south around Point Piños. This difference in the source waters for the interior of the bay is quite important from the ecological perspective. During upwelling, most of the bay water originates from the north and is cut off from the California Current by the cold equatorward jet. In contrast, wind relaxations bring warm, salty water from the south into the bay and allow greater mixing with the offshore waters. This introduces offshore larvae to the nearshore zone, and just a few large events of this type may have important consequences for successful recruitment in the bay [*Roughgarden et al.*, 1991].

[49] Comparison of Figures 4, 5, 8, 12, and 13 shows that while the major circulation patterns produced by the model are approximately correct, the model was less successful at estimating the absolute sea surface temperature. A statistical comparison indicates that the model did a better job of estimating the SST during upwelling events than during relaxations. During upwelling events, the model exhibited less "dynamic range" than the observations: The coldest water in the upwelling plume was colder and the warmest water in the NE corner of the bay was warmer in the observations than the model. During the relaxations, the model consistently underestimated the SST everywhere. During 27–29 August, the spatially averaged model-data differences had a mean of 0.87°C with a standard deviation of 0.27°C over the entire aircraft domain. During the exceptionally calm final two days, the mean model-data differences were 2.53°C with a standard deviation of 0.22°C. The differences were greatest where the thermocline was shallow and the solar insolation was large, that is, in the NE corner of the bay all the time and the entire bay during periods of calm winds and weak mixing.

5. Discussion

[50] The power of the model lies in its ability to generate additional information not revealed by the aircraft such as surface salinity distributions and subsurface currents and water mass properties. Surface salinity distributions were calculated using the ICON model to match the surface temperature distributions of Figures 12 and 13, but displaying the entire ICON domain (Figure 14). Since the surface salinity distribution is a more conservative tracer, it is a better indicator of the water mass structure than the surface temperature fields, and shows the origins of the water in the Monterey Bay. Four panels have been chosen to represent the upwelling and relaxation periods. On 17 August (Figure 14a), the upwelling centers at Point Sur and Año Nuevo are just as obvious in salinity (high) as temperature (low). Low salinity (<33.05) water entered the domain offshore at the northern boundary and nearshore along the southern boundary (<33.30), a result of coupling with the larger-scale PWC model. These features represent the equatorward flowing California Current (CC) and nearshore poleward current respectively. The nearshore poleward flow at the surface is sometimes referred to as the Davidson Current in the fall. The low salinity water from the north was held well offshore by the equatorward jet across the mouth of the bay, and water from the south was blocked by the Point Sur filament which extended well offshore on 17 August. Thus most of the surface water in the bay was high salinity (>33.55) water originating from the northern upwelling center. By 20 August (Figure 14b), under continued upwelling favorable conditions, the low-salinity water offshore continued to spread southward (past buoy M2) and most of the bay was filled with high salinity water. The situation in the southern sector of the region changed little, although there was slightly saltier water at Point Sur than on the 17 August, indicating greater upwelling there as the wind stress continued.

[51] The California Current water reached its maximum southern extent on 27 August at the end of the extended upwelling period (Figure 14c). High salinity water remained close to the coast near Point Sur but the offshore portion of the Point Sur filament had been mostly mixed away. During the subsequent poleward wind event from the 28 August to 1 September, the low salinity CC water offshore was advected onshore and poleward and entered the Monterey Bay near Point Piños. The nearshore water from along the south coast also advected swiftly northward and into the bay around the point. Both water masses were present in the bay itself by 31 August (Figure 14d). Thus the bay contained

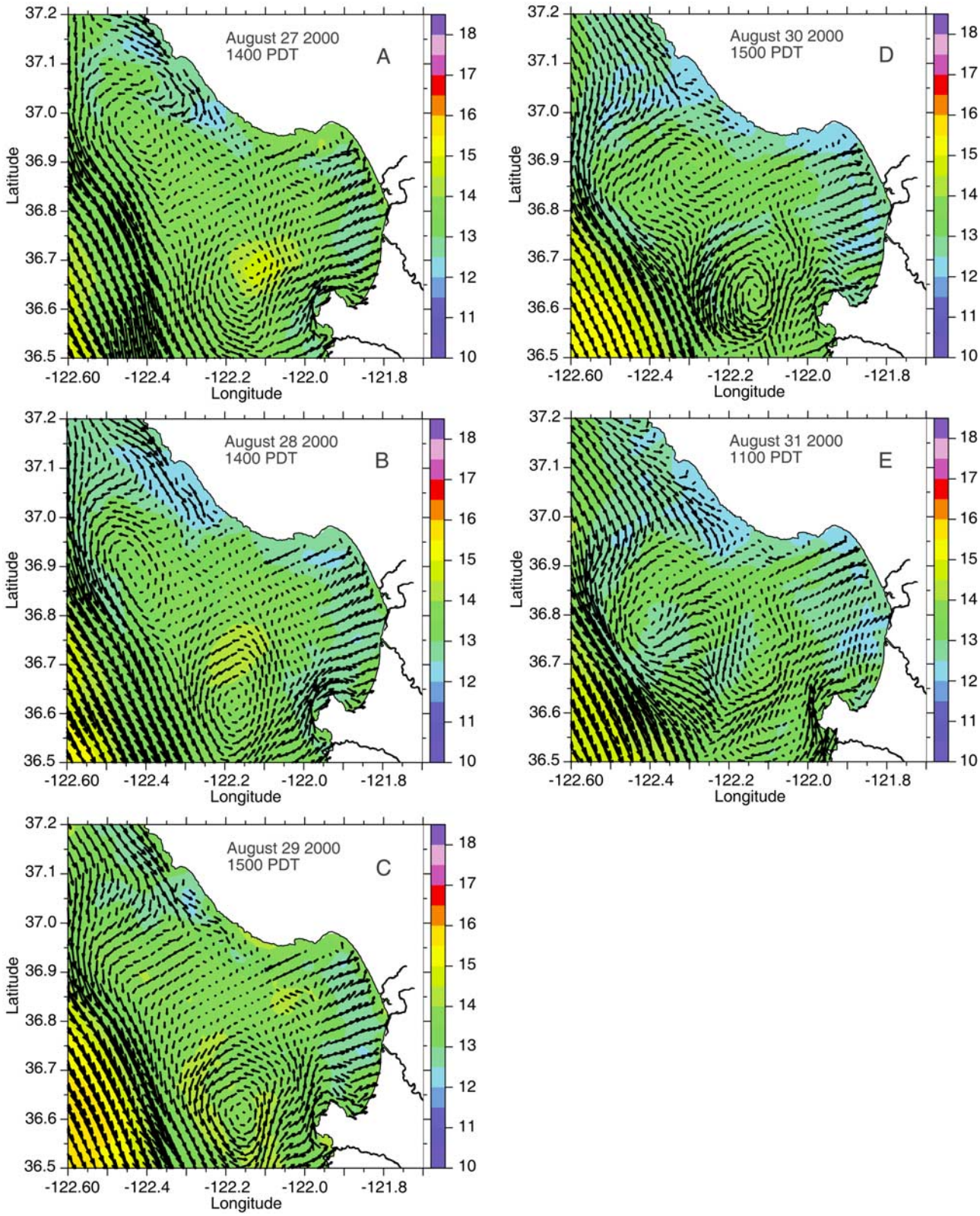

Figure 13. Surface currents and sea surface temperature from the ICON model on 27–31 August 2000. The scales are the same as those used for the observations in Figures 4, 5, and 8.

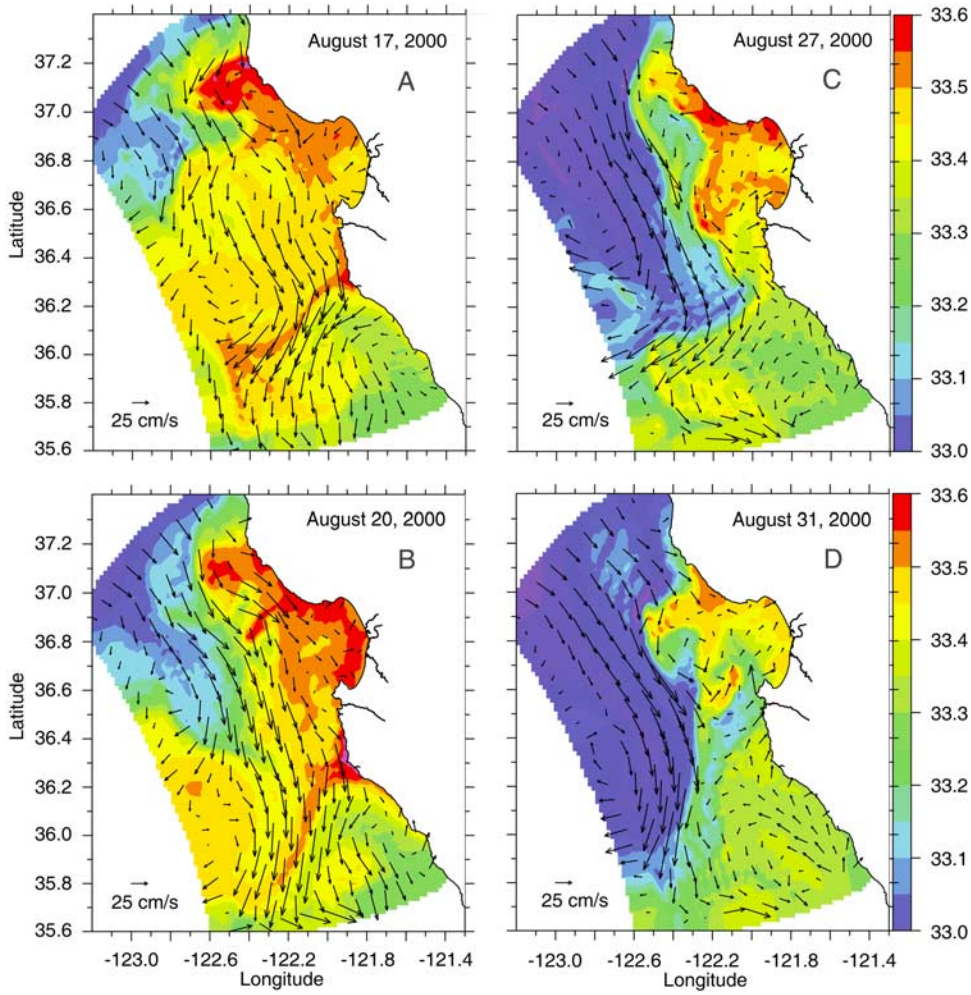

Figure 14. Surface salinity and velocity vectors for the entire ICON model domain from (a) 17 August, (b) 20 August, (c) 27 August, and (d) 31 August 2000.

lower salinity, nonupwelled surface water during the major relaxation event, which came from both offshore and the south.

[52] The model salinity and currents at 100 m provide a better indication of the importance of the local topography in controlling these features (Figure 15). The primary subsurface feature of interest is the poleward-flowing California Undercurrent (CUC), whose core is generally found between 100 and 150 m depth in this region [*Ramp et al.*, 1997; *Garfield et al.*, 1999]. The ICON model currents and salinities from 100 m depth clearly show the strong poleward CUC advecting the high (at that depth) salinity water northward along the coast south of Point Sur. This northward flow was also connected to the northward flow originating at the southern open boundary of the ICON domain and was generated by the coupling to the larger-scale PWC model. During upwelling however, this current did not reach Monterey Bay, but rather turned offshore near 36.2 °N and headed southwest along the Sur Ridge (Figures 15a and 15b). The model salinity over the Monterey Bay Canyon was higher on 20 than 17 August possibly the result of continued coastal upwelling which does reach 100 m during strong events. On 27 August, a very strong jet formed near 36.1°N, 122.2°W in the region where the poleward CUC collided with the equatorward CC (Figure 15c). This process likely contributed to the filament formation process so often observed there in satellite remote sensing products. At the height of the relaxation, the CUC crossed the ridge and continued north. As it did so, the current entrained fresher (S = 33.70 in the figure) water from offshore and transported it toward the northeast along its northwestern edge (Figure 15d). This entrained water entered the deeper portion of the Monterey Bay on 31 August, resulting in salinities in the canyon which were lower than during the upwelling events. Note that since much of the bay is a broad, shallow shelf, the area/volume of the bay is much reduced at 100 m. This is clearly a very complex region where the CC and CUC interact with the Monterey Canyon topography, and more focused field studies would be warranted there.

6. Summary

[53] The circulation along the central California coast, including the Monterey Bay, was studied during August 2000 using a combination of airborne, in situ, and shore-based HF radar techniques. The aircraft flew approximately daily from 17 to 31 August subject to the vagaries of

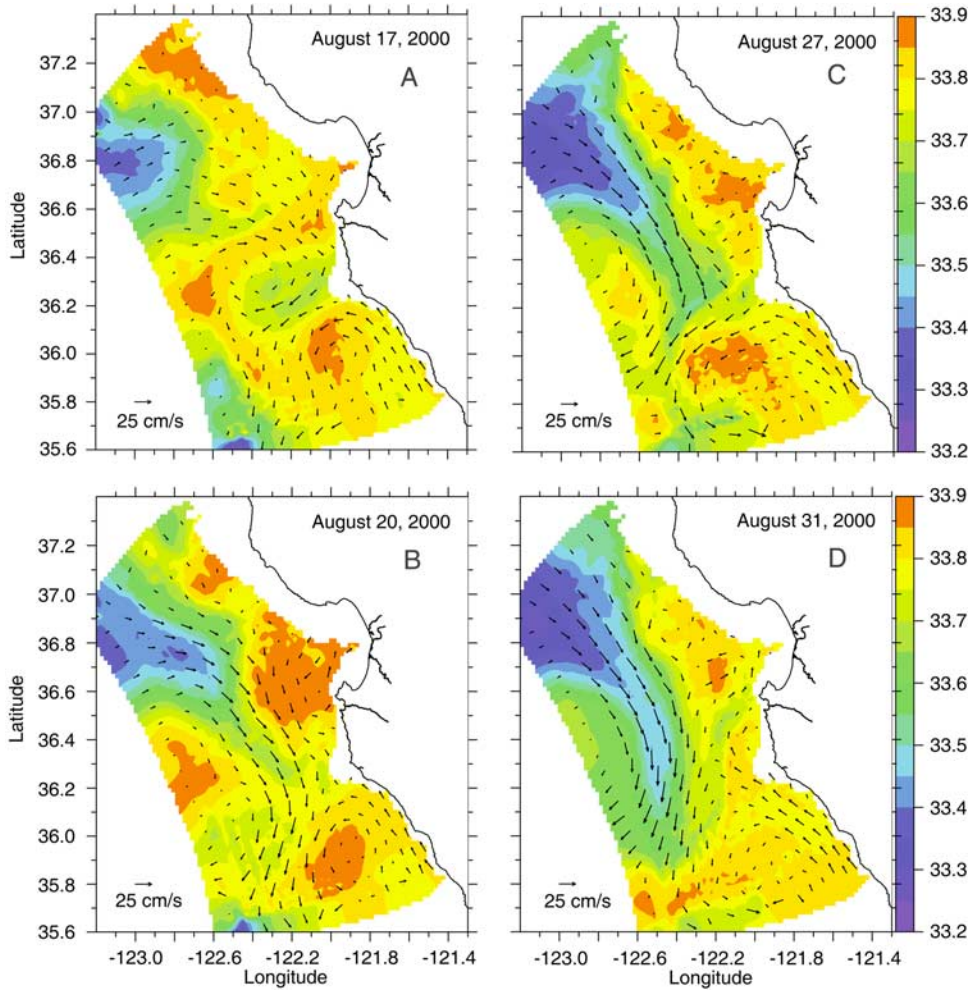

Figure 15. Salinity and current vectors at 100 m depth for the entire ICON model domain, for (a) 17 August, (b) 20 August, (c) 27 August, and (d) 31 August 2000.

weather and pilot availability, and covered most of the bay out to 122.5°W. The HF radar and ADCP time series were continuous, with the radar sampling at hourly intervals and the ADCP at 1 min intervals to assess the high-frequency internal wave variability. The observation period captured two extended upwelling events separated by two briefer periods of poleward or weak winds.

[54] The upwelling events were characterized by the appearance of cold, salty water at Point Año Nuevo at the north end of the bay which subsequently spread southward across the mouth of the bay as the winds continued. The primary difference between the 10-day event and the 4-day event was the extent of this southward spreading. Sustained winds of 10 m s^{-1} or so need to blow for on the order of a week before the upwelling filament will spread significantly southward. On 17 August during the first upwelling event, a hot, dry atmospheric jet was observed above the oceanic jet with approximately the same spatial scales. This feature may contribute to the southward spreading of the filament and/or enhanced mixing beneath the atmospheric jet. The circulation in the bay itself was cyclonic during the upwelling events, as determined by the HF radar vectors and the ADCP. The flow over the northern continental shelf was mostly toward the northwest, except when the ADCP was in the cold filament, when a sheared flow was observed with surface current toward the southeast. Very warm (>16°C) water was observed in the northeast corner of the bay off Santa Cruz, in the wind shadow behind the Santa Cruz mountains. On days with both a morning and afternoon flight, the aircraft data revealed a strong sea breeze blowing onshore up the Salinas Valley in the afternoon which was completely absent in the morning. The sea breeze effect was evident in the CODAR surface currents but had little impact on the position of the major mesoscale features.

[55] During the downwelling/relaxation events, the surface current and temperature response was dominated by the onshore translation of the Monterey Bay Eddy and by local surface heating in the bay itself. From 27 to 31 August, the MBE moved onshore and southward at about 5 km d^{-1}. The surface current vectors from buoy M2, and the HF radar where available, paralleled the thermal front consistent with the anticyclonic circulation and geostrophic flow. Surface temperatures reached record highs in the bay during two unusually calm days on 30–31 August. This phenomenon, which was sensed by the aircraft, represented a surface skin layer effect which was undetectable in the moored buoys. Surface currents in the bay itself remained counterclockwise, but were more barotropic than during upwelling

events. The water entering the bay in the south however came from offshore and the south and was 0.4 psu fresher than during upwelling events.

[56] The ICON model, a nested, data assimilating, sigma coordinate model, was used to simulate the upwelling and relaxation events and calculate the subsurface current and density fields. The model was forced at the boundaries by the Pacific West Coast (PWC) model and at the surface by the 9 km COAMPS heat fluxes and winds. The model surface currents and temperatures were first compared to the HF radar vectors and aircraft SST, and subsequently used to study the surface and subsurface water mass properties in and around the Monterey Bay.

[57] The ICON model did a good job of producing the dominant current and temperature patterns in the bay, including the southward flowing upwelling filament, the movement of the Monterey Bay Eddy, the poleward flow off Point Sur, and the sense of the circulation in the bay. The model did less well producing the absolute SST, underestimating the maxima in the bay and overestimating the minima offshore. The model did better during upwelling events than during calm/downwelling events. The difficulty seemed to stem from the atmospheric heat fluxes and small-scale stratification and mixing processes in the upper few meters of the water column.

[58] The model salinity fields at the surface and 100 m levels over a slightly larger domain were particularly useful in identifying the water masses entering the bay during upwelling and relaxation conditions. During upwelling, the bay was filled with higher-salinity water stemming from the Point Año Nuevo upwelling center to the north: During downwelling, the source water for both the surface and 100 m levels was the colder, fresher California Current water offshore, which had advected southward well past Point Piños during the previous upwelling event. This water then moved northeast onshore during the relaxation event.

[59] **Acknowledgments.** This work was supported by the Office of Naval Research Ocean Modeling and Prediction (Code 322OM) and Biological and Chemical Oceanography (Code 322BC) Programs as part of the Autonomous Ocean Sensing Network (AOSN) program. The Navajo aircraft was supported while in Monterey by the NPS Center for Interdisciplinary Remotely-Piloted Aircraft Studies (CIRPAS). The authors thank Bob Bluth, Haf Jonnson, and Jeff Reid for their contributions to the data collection and processing. Mooring RT was expertly prepared, deployed, and recovered by Marla Stone aboard the R/V *Point Sur* and the R/V *Shana Rae*. We thank Sergio DeRada and Stephanie Anderson for processing atmospheric forcing and open boundary conditions for the ICON and PWC models. Computer time for the numerical simulations was provided through a grant from the Department of Defense High Performance Computing Initiative. This manuscript is NRL contribution JA/7331.

References

Barrick, D. E., M. W. Evans, and B. L. Weber (1977), Ocean surface currents mapped by radar, *Science*, *198*, 138–144.

Bigelow, H. B., and M. Leslie (1930), Reconnaissance of the waters and plankton of Monterey Bay, July, 1928, *Bull. Museum Comp. Zool. Harvard Coll.*, *70*, 427–581.

Blumberg, A., and G. L. Mellor (1987), A description of a three-dimensional coastal ocean circulation model, in *Three Dimensional Coastal Models*, *Coastal Estuar. Ser.*, vol. 4, edited by N. S. Heaps, 1–16, AGU, Washington, D. C.

Bolin, R. L., and D. P. Abbott (1963), Studies on the marine climate and phytoplankton of the central coastal area of California, 1954–1960, *Calif. Coop. Fish. Invest.*, *9*, 23–45.

Breaker, L. C., and R. P. Gilliland (1981), A satellite sequence on upwelling along the California coast, in *Coastal Upwelling*, *Coastal Estuar. Ser.*, vol. 1, edited by F. A. Richards, pp. 87–94, AGU, Washington, D. C.

Breaker, L. C., and C. N. K. Mooers (1986), Oceanic variability off the central California coast, *Prog. Oceanogr.*, *17*, 61–135.

Brink, K. H., R. C. Beardsley, P. P. Niiler, M. R. Abbott, A. Huyer, S. R. Ramp, T. P. Stanton, and D. Stuart (1991), Statistical properties of near surface flow in the California coastal transition zone, *J. Geophys. Res.*, *96*, 14,693–14,706.

Chelton, D. B. (1984), Seasonal variation of alongshore geostrophic velocity off central California, *J. Geophys. Res.*, *89*, 3473–3486.

Emery, W. J., and R. E. Thomson (1998), *Data Analysis Methods in Physical Oceanography*, 634 pp., Elsevier, New York.

Garfield, N., C. A. Collins, R. G. Paquette, and E. Carter (1999), Lagrangian exploration of the California Undercurrent, 1992–1995, *J. Phys. Oceanogr.*, *29*, 560–583.

Graham, W. M. (1993), Spatio-temporal scale assessment of an "upwelling shadow" in northern Monterey Bay, California, *Estuaries*, *16*, 83–91.

Graham, W. M., and J. L. Largier (1997), Upwelling shadows as nearshore retention sites: The example of northern Monterey Bay, *Cont. Shelf Res.*, *17*, 509–532.

Haidvogel, D. B., J. Blanton, J. C. Kindle, and D. R. Lynch (2000), Coastal ocean modeling: Processes, and real-time systems, *Oceanography*, *13*, 35–46.

Hodur, R. M., J. Pullen, J. Cummings, X. Hong, J. D. Doyle, P. J. Martin, and M. A. Rennick (2002), The Coupled Ocean/Atmospheric Mesoscale Prediction System (COAMPS), *Oceanography*, *15*, 88–98.

Kindle, J. C., R. Hodur, S. deRada, J. Paduan, L. K. Rosenfeld, and F. P. Chavez (2002), A COAMPS™ reanalysis for the eastern Pacific: Properties of the diurnal sea breeze along the central California coast, *Geophys. Res. Lett.*, *29*(24), 2203, doi:10.1029/2002GL015566.

Kundu, P. K. (1976), Ekman veering observed near the ocean bottom, *J. Phys. Oceanogr.*, *6*, 238–242.

Lentz, S. J. (1987), A description of the 1981 and 1982 spring transitions over the northern California shelf, *J. Geophys. Res.*, *92*, 1545–1567.

Lipa, B. J., and D. E. Barrick (1983), Least-squares method for the extraction of surface currents from CODAR Crossed-loop data: Application at ARSLOE, *IEEE J. Oceanic Eng.*, *8*, 226–253.

Nelson, C. S. (1977), Wind stress and wind stress curl over the California Current, *NOAA Tech. Rep. NMFS, SSRF-714*, 89 pp.

Noble, M. A., and S. R. Ramp (2000), Subtidal currents over the central California slope: Evidence for offshore veering of the undercurrent and for direct, wind-driven slope currents, *Deep Sea Res., Part II*, *47*, 871–906.

Paduan, J. D., and M. S. Cook (1997), Mapping surface currents in Monterey Bay with CODAR-type HF radars, *Oceanography*, *10*, 49–52.

Paduan, J. D., and L. K. Rosenfeld (1996), Remotely sensed surface currents in Monterey Bay from shore-based HF radar (Coastal Ocean Dynamics Application Radar), *J. Geophys. Res.*, *101*, 20,669–20,686.

Paduan, J. D., and I. Shulman (2004), HF radar data assimilation in the Monterey Bay area, *J. Geophys. Res.*, *109*, C07S09, doi:10.1029/2003JC001949.

Petruncio, E. T. (1993), Characterization of tidal currents in Monterey Bay from remote and in-situ measurements, M.S. thesis, 113 pp., Naval Postgraduate School, Monterey, Calif.

Petruncio, E. T., L. K. Rosenfeld, and J. D. Paduan (1998), Observations of the internal tide in Monterey Canyon, *J. Phys. Oceanogr.*, *28*, 1873–1903.

Petruncio, E. T., J. D. Paduan, and L. K. Rosenfeld (2002), Numerical simulations of the internal tide in a submarine canyon, *Ocean Modell. 4*, Hooke Inst. Oxford Univ., Oxford, England, pp. 221–248.

Pierce, S. D., R. L. Smith, P. M. Kosro, J. A. Barth, and C. D. Wilson (2000), Continuity of the poleward undercurrent along the eastern boundary of the mid-latitude north Pacific, *Deep Sea Res., Part II*, *47*, 811–829.

Ramp, S. R., and C. L. Abbott (1998), The vertical structure of currents over the continental shelf off Point Sur, CA, during spring 1990, *Deep Sea Res., Part II*, *45*, 1443–1470.

Ramp, S. R., R. W. Garwood, C. Davis, and R. L. Snow (1991), Surface heating and patchiness in the coastal ocean off central California during a wind relaxation event, *J. Geophys. Res.*, *96*, 14,947–14,958.

Ramp, S. R., L. K. Rosenfeld, T. D. Tisch, and M. R. Hicks (1997), Moored observations of the current and temperature structure over the continental slope off central California: 1. A basic description of the variability, *J. Geophys. Res.*, *102*, 22,877–22,902.

Rhodes, R. C., et al. (2001), Navy real-time global modeling systems, *Oceanography*, *15*, 29–43.

Rochford, P. A., and I. Shulman (2000), Boundary conditions in the Pacific West Coast Princeton Ocean Model of CoBALT, *NRL Tech. Rep., NRL/MR/7330–00–8245*, 18 pp.

Rosenfeld, L. K., F. B. Schwing, N. Garfield, and D. E. Tracy (1994), Bifurcated flow from an upwelling center: A cold water source for Monterey Bay, *Cont. Shelf Res.*, *14*, 931–964.

Roughgarden, J., J. Pennington, D. Stoner, S. Alexander, and K. Miller (1991), Collisions of upwelling fronts with the intertidal zone: The cause of recruitment pulses in barnacle populations of central California, *Acta Ecol.*, *12*, 35–51.

Shulman, I., C. R. Wu, J. D. Paduan, J. K. Lewis, L. K. Rosenfeld, and S. R. Ramp (2001), High frequency radar data assimilation in the Monterey Bay, in *Estuarine and Coastal Modeling, Proceedings from Seventh International Conference*, edited by M. L. Spaulding, pp. 434–446, Am. Soc. of Civ. Eng., New York.

Shulman, I., C. R. Wu, J. K. Lewis, J. D. Paduan, L. K. Rosenfeld, J. C. Kindle, S. R. Ramp, and C. A. Collins (2002), High resolution modeling and data assimilation in the Monterey Bay Area, *Cont. Shelf Res.*, *22*, 1129–1151.

Tisch, T. D., S. R. Ramp, and C. A. Collins (1992), Observations of the geostrophic current and water mass characteristics off Point Sur, California from May 1988 through November 1989, *J. Geophys. Res.*, *97*, 12,535–12,556.

Wickham, J. B., A. A. Bird, and C. N. K. Mooers (1987), Mean and variable flow over the central California continental margin, 1978–1980, *Cont. Shelf Res.*, *7*, 827–849.

Winant, C. D., R. C. Beardsley, and R. E. Davis (1987), Moored wind, temperature, and current observations made during Coastal Ocean Dynamics Experiments 1 and 2 over the northern California continental shelf and upper slope, *J. Geophys. Res.*, *92*, 1569–1604.

F. L. Bahr, J. D. Paduan, and S. R. Ramp, Department of Oceanography, Naval Postgraduate School, Monterey, CA 93943, USA. (sramp@nps.edu)

F. Chavez, Monterey Bay Aquarium Research Institute, 7700 Sandholdt Road, Moss Landing, CA 95039, USA.

J. Kindle and I. Shulman, Oceanography Division, Naval Research Laboratory, Stennis Space Center, MS 39529, USA.